

Composite localized modes in discretized spin-orbit-coupled Bose-Einstein condensates

Petra P. Beličev¹, Goran Gligorić¹, Jovana Petrovic¹,
Aleksandra Maluckov¹, Ljupčo Hadžievski¹ and Boris A.
Malomed²

Abstract. We introduce a discrete model for binary spin-orbit-coupled (SOC) Bose-Einstein condensates (BEC) trapped in a deep one-dimensional optical lattice. Two different types of the couplings are considered, with spatial derivatives acting inside each species, or between the species. The discrete system with inter-site couplings dominated by the SOC, while the usual hopping is negligible, *emulates* condensates composed of extremely heavy atoms, as well as those with opposite signs of the effective atomic masses in the two components. Stable localized composite states of miscible and immiscible types are constructed. The effect of the SOC on the immiscibility-miscibility transition in the localized complexes, which emulates the phase transition between insulating and conducting states in semiconductors, is studied.

PACS numbers: 05.45.Yv; 03.75.Lm; 03.75.Mn

¹Vinča Institute of Nuclear Sciences, University of Belgrade, P. O. B. 522,11001 Belgrade, Serbia

²Department of Physical Electronics, School of Electrical Engineering, Faculty of Engineering, Tel Aviv University, Tel Aviv 69978, Israel

E-mail: petrab@vin.bg.ac.rs

Keywords: spin-orbit coupling, two component BEC, miscibility-immiscibility transition, discrete soliton complexes

1. Introduction

Recently, the use of ultracold quantum gases – atomic Bose-Einstein condensates (BEC) and fermion gases alike – for simulating fundamental effects originating in condensed-matter physics has drawn much interest [1]. One of these effects is the spin-orbit coupling (SOC) which links the electron spin to its motion in semiconductors. The SOC of the Dresselhaus [2] and Rashba [3] types plays a major role in many phenomena and applications, including spin and anomalous Hall effects [4], topological insulators [5], spintronics [6, 7], spin-based quantum computations [8], etc. In contrast to the complex situations found in solids, the “synthetic” SOC, induced by appropriate laser illumination of atomic gases in the combination with a magnetic field, can be precisely

controlled in the experiment [9, 10, 11, 12]. Furthermore, unlike the electron spin, the pseudo-spin of laser-dressed atoms is not constrained by fundamental symmetries, which gives rise to a variety of settings unavailable in solids, such as new exotic superfluids [13]. The theoretical description of SOC effects in BEC is also much simpler than in solids [9, 14, 15]. Therefore, studies of the SOC in BEC, as well as in fermionic gases [16, 17], have become a vast research area, see Ref. [18] for a brief review.

SOC in solid state is manifested by electrons moving in static electric fields [19, 20, 21]. The coupling results from the Zeeman interaction between the magnetic moment of the electron, aligned with its spin, and the magnetic field appearing in the reference frame moving along with the electron. To link this setting to the atomic gas, the electron's spinor wave function is mapped into a pseudo-spinor mean-field wave function of the binary BEC in ^{87}Rb , which contains atoms in two different states "dressed" by appropriate laser fields. In particular, making use of the electronic ground-state $5S_{1/2}$, $F = 1$ and $F = 2$ hyperfine manifolds, one can start with the set of four states, $|F, m_F\rangle = |2, 0\rangle, |1, -1\rangle, |1, 0\rangle, |2, 1\rangle$, which are cyclically coupled by four strong fields directed along diagonals in the (x, y) plane, with the magnetic field applied along z . As shown in [9], by means of an appropriate unitary transformation, which dresses the original atomic states, this setting may be described by a combination of the Rashba and Dresselhaus Hamiltonians, with independently adjustable coefficients, α and β , acting on a set of two dressed states, that emulate the spin-up and spin-down polarizations of electrons in the semiconductor:

$$\hat{H}_1 = \alpha (\sigma_x \hat{p}_y - \sigma_y \hat{p}_x) + \beta (\sigma_x \hat{p}_y + \sigma_y \hat{p}_x), \quad (1)$$

where $\sigma_{x,y}$ are the Pauli matrices, and $\hat{p}_{x,y}$ are operators of the respective momentum components.

In the seminal experimental work [10], a different setting was implemented in the condensate of ^{87}Rb : a pair of Raman laser beams with wavelength λ , shone along the same diagonal directions in the (x, y) plane and with the same vertical orientation of the magnetic field as mentioned above, were used to couple two states, $|\psi^+\rangle = |F = 1, m_F = 0\rangle$ and $|\psi^-\rangle = |F = 1, m_F = -1\rangle$ (the third one, $|F = 1, m_F = +1\rangle$, which belongs to the same manifold, is far detuned from this pseudo-spinor set). The original Hamiltonian of the system includes the kinetic energy of atoms, Zeeman terms, and inter-component coupling terms modulated by factors $\exp(\pm 4\pi i x/\lambda)$. The transformation of this Hamiltonian by unitary matrix $U = \exp(2\pi i \sigma_z x/\lambda)$ makes it possible to eliminate the explicit x -dependence, simultaneously generating the effective SOC term,

$$\hat{H}_2 = \gamma \sigma_z \hat{p}_x, \quad (2)$$

due to the noncommutivity of U and term $\hat{p}_x^2/(2m)$ in the kinetic-energy operator. Further, the pseudo-spin rotation can make H_2 equivalent to the combination of the Rashba and Dresselhaus couplings with equal strength, i.e., a particular case of the generic Hamiltonian (1).

The interplay of the SOC with intrinsic collisional nonlinearity of the pseudo-spinor BEC was recently considered too, in many theoretical works. In particular, it was

demonstrated the new ground-state phases (stripes, phase separation, etc.) can be created in a such nonlinear two-component systems [22], as well as tricritical points [23], solitons of different types [24, 25, 26, 27], including two-dimensional solitons with embedded vorticity [28, 29, 30], and vortex lattices [31]. New topological excitations emerge in spin-orbit-coupled fermionic gases too [17]. SOC gives rise to other noteworthy phenomena when combined with an optical-lattice (OL) potential: flattening of the Bloch potential [32], atomic *Zitterbewegung* [33], and new topological phases [34].

Our objective here is to derive a discrete form of the SOC-BEC model for the pseudo-spinor condensate trapped in a deep OL potential, and then construct discrete solitons specific to this model. Especially interesting is the regime in which the inter-site coupling is dominated by SOC, while the usual hopping may be neglected. It gives rise to a previously unknown discrete model that makes it possible to emulate the SOC in BEC composed of infinitely heavy atoms, as well as emulate binary condensates with opposite signs of effective atomic masses (dynamics of trapped SOC BEC featuring an infinite effective mass in some special cases was recently addressed in non-discrete settings both experimentally [12] and theoretically [15]).

We also investigate the immiscibility-miscibility (IM) transition induced by the SOC in localized pseudo-spin complexes. In this connection, it is relevant to mention that, in the absence of linear couplings between the components, the hyperfine states in ^{87}Rb are immiscible, although being close to the miscibility threshold [35, 36, 37]. Previously elaborated proposals to achieve a tunable immiscibility-miscibility transition relied on the adjustment of the scattering length via the Feshbach resonance, controlled by magnetic [38, 39] or optical [40, 41] fields, or on linear coupling between the different atomic species imposed by a radio-frequency field [42, 43]. The SOC imposes its specific linear mixing via spatial gradients of the wave functions, thus offering a new way to induce the immiscibility-miscibility transition.

The SOC model, written in terms of coupled discrete Gross-Pitaevskii equations (GPEs), is introduced in Section II. Results for discrete bright-soliton complexes in this system and their stability, as well as for the effect of the SOC on the immiscibility-miscibility transition in the binary condensate, are presented in Section III. The paper is concluded by Section IV.

2. The model

2.1. Basic equations

We consider the BEC composed of atoms in different hyperfine ground states corresponding, as said above, to $F = 1$ [10] or $F = 1, 2$ [9]. The states are coupled by two [10] or four [9] Raman laser beams shone at angle $\pi/4$ in the $x - y$ plane with respect to the system's axis x , with the dc magnetic field applied along z . These settings induce the SOC in the basis of two dressed states, which emulate the spin up and down components. In the presence of the OL potential, V_{OL} , the mean-field dynamics of the

BEC is governed by the GPE written in the spinor form:

$$i\hbar\frac{\partial\Psi}{\partial t} = \left[\frac{\hat{p}^2}{2m} + V_{\text{OL}} + \hat{H}_{\text{SOC}} + \hat{H}_{\text{mix/spl}} + H_{\text{int}} \right] \Psi, \quad (3)$$

where $\Psi = (\psi^+, \psi^-)^T$ is the normalized spinor wave function in the dressed-state representation, and $\hat{p}^2/(2m)$ represents the kinetic energy of the quasi-1D condensate.

According to the above discussion, the Hamiltonian term (2), which accounts for the SOC in the setting similar to that which was experimentally realized in [10], amounts to

$$\hat{H}_{\text{SOC}} = -i\frac{\hbar^2}{m}\kappa\sigma_z\frac{\partial}{\partial x}, \quad (4)$$

where κ is the SOC strength. In this case, we assume that the condensate is subject to tight confinement in the y and z directions, hence \hat{p}^2 in Eq. (3) may be replaced by \hat{p}_x^2 . On the other hand, starting from the more general SOC Hamiltonian (1), and assuming the tight confinement in the (z, x) plane, i.e., keeping only \hat{p}_y in \hat{p}^2 in Eq. (3) and in (1), the SOC Hamiltonian amounts to

$$\hat{H}_{\text{SOC}} = -i\frac{\hbar^2}{m}\kappa\sigma_x\frac{\partial}{\partial y}, \quad (5)$$

with respective strength κ .

The Hamiltonian term (4) implies that the spatial derivatives accounting for the SOC act inside of each dressed state (we call this system an intra-SOC one), while the term (5) couples different dressed states by the derivatives (to be called the inter-SOC system). In the former and latter cases, the unconfined coordinate is denoted as x and y , respectively. The commutation of the SOC terms in the Hamiltonian with the respective coordinate gives rise to what may be considered as anomalous velocity, and effects produced by the SOC terms, such as the immiscibility-miscibility transition (see below) may be accordingly understood as mixing caused by this velocity.

Further, the linear-mixing or splitting terms of the Hamiltonian, which are induced by the magnetic field, are represented, severally, by $\hat{H}_{\text{mix}} = \hbar\Omega\sigma_x$ and $\hat{H}_{\text{spl}} = \hbar\Omega\sigma_z$ in the intra- and inter-SOC systems, where Ω is, respectively, the Rabi coupling or Zeeman splitting between the two wave-function components. Lastly, H_{int} accounts for the collisional intra- and inter-component interactions in the BEC.

The fragmentation of the condensate in the deep OL potential into droplets coupled by tunnelling across barriers separating local potential wells leads to the replacement of the continuous GPEs by their discrete counterparts, which can be performed in essentially the same way (using the tight-binding approximation) as it was elaborated for the single-component BEC [44, 50]. Thus, adopting the units where $\hbar = 1$, $m = 1$, we arrive at a system of two discrete GPEs for the (pseudo-) spinor wave function, $\Psi_n = (\psi_n^+, \psi_n^-)^T$, where n is the discrete coordinate, which replaces x in Eq. (4), or y in Eq. (5). The first system corresponds to the intra-SOC, cf. Eq. (4), with the first-order finite-difference derivatives acting separately on each component:

$$i\frac{\partial\psi_n^+}{\partial t} = -C(\psi_{n+1}^+ + \psi_{n-1}^+) - i\kappa(\psi_{n+1}^+ - \psi_{n-1}^+) + (\gamma_1|\psi_n^+|^2 + \beta|\psi_n^-|^2)\psi_n^+ - \Omega\psi_n^-,$$

$$i\frac{\partial\psi_n^-}{\partial t} = -C(\psi_{n+1}^- + \psi_{n-1}^-) + i\kappa(\psi_{n+1}^- - \psi_{n-1}^-) + (\beta|\psi_n^+|^2 + \gamma|\psi_n^-|^2)\psi_n^- - \Omega\psi_n^+ \quad (6)$$

The other model corresponds to the inter-SOC, in which the finite-difference derivatives mix the components, cf. Eq. (5):

$$\begin{aligned} i\frac{\partial\psi_n^+}{\partial t} &= -C(\psi_{n+1}^+ + \psi_{n-1}^+) + i\kappa(\psi_{n+1}^- - \psi_{n-1}^-) + (\gamma_1|\psi_n^+|^2 + \beta|\psi_n^-|^2)\psi_n^+ - \Omega\psi_n^+, \\ i\frac{\partial\psi_n^-}{\partial t} &= -C(\psi_{n+1}^- + \psi_{n-1}^-) + i\kappa(\psi_{n+1}^+ - \psi_{n-1}^+) + (\beta|\psi_n^+|^2 + \gamma|\psi_n^-|^2)\psi_n^- + \Omega\psi_n^+ \end{aligned} \quad (7)$$

In either system κ is the rescaled SOC strength, $\gamma, \gamma_1 < 0$ and $\beta < 0$ are, respectively, coefficients of the intra- and inter-component interactions, which we assume here to be attractive, and Ω is the Rabi-coupling or Zeeman-splitting frequency in Eqs. (6) and (7), respectively. The nonlinearity coefficients are normalized by setting $\gamma_1 \equiv -1$. The remaining free parameters are κ, β, γ , and Ω , along with the inter-site hopping coefficient, $C > 0$.

It is well known that the discrete equation with repulsive on-site nonlinearity can be transformed into its counterpart with the attractive interaction by means of the staggering transformation followed by the complex conjugation:

$$\psi_n \equiv (-1)^n \tilde{\psi}_n^*, \quad (8)$$

where the asterisk stands for the complex conjugate. If the underlying nonlinearity is repulsive, the transformation will invert the original signs of γ_1, γ and β , while the sign of the SOC coefficient, κ , will not change.

Each system conserves two quantities, that are written here for infinite lattices: the norm,

$$P = \sum_n (|\psi_n^+|^2 + |\psi_n^-|^2), \quad (9)$$

and Hamiltonian, which is

$$\begin{aligned} H &= \sum_n \left\{ -C(\psi_n^{+*}\psi_{n+1}^+ + \psi_n^{-*}\psi_{n+1}^-) - i\kappa(\psi_n^{+*}\psi_{n+1}^+ - \psi_n^{-*}\psi_{n+1}^-) \right. \\ &\quad \left. + \frac{1}{4}(\gamma_1|\psi_n^+|^4 + \gamma|\psi_n^-|^4) + \frac{\beta}{2}|\psi_n^+|^2|\psi_n^-|^2 - \Omega\psi_n^{+*}\psi_n^- \right\} + \text{c.c.} \end{aligned} \quad (10)$$

for the intra-SOC system (6), and

$$\begin{aligned} H &= \sum_n \left\{ -C(\psi_n^{+*}\psi_{n+1}^+ + \psi_n^{-*}\psi_{n+1}^-) + i\kappa\psi_n^{+*}(\psi_{n+1}^- - \psi_{n-1}^-) \right. \\ &\quad \left. + \frac{1}{4}(\gamma_1|\psi_n^+|^4 + \gamma|\psi_n^-|^4) + \frac{\beta}{2}|\psi_n^+|^2|\psi_n^-|^2 - \frac{\Omega}{2}(|\psi_n^+|^2 - |\psi_n^-|^2) \right\} + (\mathbf{11}) \end{aligned}$$

for the inter-SOC system (7), where c.c. stands for the complex-conjugate expression.

2.2. Stationary solutions

Stationary solutions for the above systems are sought for as $\psi_n^+ = A_n \exp(-i\mu t)$ and $\psi_n^- = B_n \exp(-i\mu t)$, where μ is the chemical potential. The set of stationary equations

following from Eqs. (6) is

$$\begin{aligned}\mu A_n &= -C(A_{n+1} + A_{n-1}) - i\kappa(A_{n+1} - A_{n-1}) + (\gamma_1|A_n|^2 + \beta|B_n|^2)A_n - \Omega B_n, \\ \mu B_n &= -C(B_{n+1} + B_{n-1}) + i\kappa(B_{n+1} - B_{n-1}) + (\beta|A_n|^2 + \gamma|B_n|^2)B_n - \Omega A_n\end{aligned}$$

and its counterpart following from Eq. (7) is

$$\begin{aligned}\mu A_n &= -C(A_{n+1} + A_{n-1}) + i\kappa(B_{n+1} - B_{n-1}) + (\gamma_1|A_n|^2 + \beta|B_n|^2)A_n - \Omega A_n, \\ \mu B_n &= -C(B_{n+1} + B_{n-1}) + i\kappa(A_{n+1} - A_{n-1}) + (\beta|A_n|^2 + \gamma|B_n|^2)B_n + \Omega B_n\end{aligned}$$

Our aim is to find stable discrete solitons for both systems, with the intra- and inter-SOC. To this end, stationary equations (12) and (13) were solved by means of a numerical algorithm based on the modified Powell minimization method [46]. Stability of so found discrete solitons was checked, in the framework of the linear stability analysis, by numerically solving the corresponding eigenvalue problem for modes of small perturbations. Finally, Eqs. (6) and (7) were directly simulated by dint of the Runge-Kutta procedure of the sixth order, [46], to verify stability properties predicted by the linear analysis. This was done by performing direct simulations with generic small random perturbations added to the initial conditions.

2.3. The dispersion relation

The search for localized solutions – here, complexes formed by discrete solitons in each BEC component – starts from the derivation of the underlying dispersion relations. To this end, we substitute $\psi_n^+ = \psi^+ \exp(i(kn - \mu t))$ and $\psi_n^- = \psi^- \exp(i(kn - \mu t))$, with wavenumber k , into the linearized version of Eqs. (6) and (7). Straightforward algebra gives rise to the following dispersion relation for both intra-SOC and inter-SOC systems:

$$\mu_{1,2} = -2C \cos k \pm \sqrt{\Omega^2 + 4\kappa^2 \sin^2 k}. \quad (14)$$

Further analysis of the dispersion relation is worded in terms of the intra-SOC model, for which discrete solitons are actually produced below.

In the absence of the linear coupling between the two components, i.e., $\Omega = 0$, Eq. (14) reduces to a straightforward generalization of the commonly known spectrum of the discrete linear Schrödinger equation. In the present case, the spectrum corresponding to $\Omega = 0$ contains the Bloch band, $|\mu_{1,2}| \leq 2\sqrt{C^2 + \kappa^2}$, sandwiched between two semi-infinite gaps. As follows from elementary analysis of Eq. (14), and shown in Fig. 1(a), the same remains qualitatively correct if the SOC is relatively weak, *viz.*, at $|\Omega| \leq 2C$. Further increase of the strength of the linear coupling between the components opens a *mini-gap* in the middle of the Bloch band, which exists at $|\Omega| > 2C$, occupying the region of

$$|\mu_{1,2}| < |\Omega| - 2C, \quad (15)$$

as shown in Fig. 1(b). Usually, mini-gaps open up in the spectrum of 1D [47] and 2D [48] *superlattices*, i.e., discrete lattices which are subjected to an additional spatially periodic modulation. A mini-gap is also present in the spectrum of the discrete coupler

introduced in Ref. [49]. In the present case, it may be understood, roughly, as a result of the precession of the pseudo-spin around the magnetic axis. Lastly, Fig. 1(c) displays the limit case of $C = 0$, when the usual inter-site hoppings are negligible in comparison with the SOC-induced linear inter-site coupling, while the semi-infinite bandgaps and the mini-gap are still present in the spectrum.

The tight-binding approximation underlying the derivation of the discrete equations takes into account only the first Bloch band, while the higher-order ones are neglected. This means that the band is sandwiched, as said above, between two semi-infinite bandgaps [see Fig. 1(a)]. In the presence of the attractive nonlinearity, the existence of fundamental (*unstaggered*) discrete solitons is expected in the lower semi-infinite gap. Solitons of this type are chiefly considered in this work. On the other hand, staggered solitons, with π -shifted fields at adjacent sites, may exist in the mini-gap [48, 49, 50]. Basic results for the latter type of the discrete solitons are briefly reported below too.

3. Results and discussion

In the following, results are chiefly presented for the intra-SOC model, based on Eq. (6). Qualitatively similar conclusions can be obtained for the inter-SOC model based on (7), which is explained by the fact that lattice solitons tend to be similar in different systems, due to the strong effect of the discretization. Recently, both 2D and 1D discrete models with the inter-SOC terms (the Rashba coupling) were considered in [30]; however, unlike the present analysis, which focuses on strongly discrete states, that work was dealing with broad discrete solitons corresponding to the quasi-continuum regime.

The discrete SOC-BEC systems support different types of bright solitons, depending on the systems' parameters. They are classified here as miscible and immiscible complexes (MC and IMC, respectively, see Fig. 2), formed of localized patterns in both components [42, 43]. We consider as miscible the localized complexes in which both stationary components (A_n and B_n) are overlapping, see Fig. 2(a). On the other hand, immiscible states are characterized by separated shapes of the two components. The numerical results demonstrate that stable IMCs are mostly formed by one component featuring two maxima and the other component with a single maximum between these two, see Fig. 2(b). It is relevant to mention that broad (quasi-continual) discrete solitons found for the inter-SOC system in [30] also feature miscible and immiscible structures, which are called, in that context, "smooth" and "striped" ones (the latter pattern demonstrates a large number of alternating local peaks of the density of the two components).

Our analysis has identified four basic types of the MC solutions, which may be built as follows (cf. Ref. [51]): in-phase on-site solitons (IPOS), $\text{Re}(A_n) \times \text{Re}(B_n) > 0$, counter-phase on-site solitons (CPOS), $\text{Re}(A_n) \times \text{Re}(B_n) < 0$, in-phase inter-site solitons (IPIS), $\text{Re}(A_n) \times \text{Re}(B_n) > 0$, and counter-phase inter-site solitons, $\text{Re}(A_n) \times \text{Re}(B_n) < 0$ (CPIS), see Fig. 3.

Considering the IMCs, various structures of the on- and inter-site types have been

found, which reflects strong sensitivity of the system to parameter values. We report here only those IMCs which may be stable, and mention scenarios of the transformation of unstable IMCs into MCs. In fact, only on-site IMCs are found to be stable in certain ranges of the parameter space.

Miscible on-site complexes of both the in-phase and counter-phase types are found to be stable over large parts of their existence region in parameter space $(\gamma, \beta, \kappa, \Omega, C)$. As mentioned above, they belong to the lower semi-infinite gap of the systems' spectra, shown in Fig. 1. IPOS complexes lose the stability only in a limited parameter area; for example, in the case of $C = 1$ they are unstable at $\beta > -1$ and $-2 < \Omega < -0.5$. In direct simulations, the instability in that area leads to spontaneous formation of breathing localized structures with a smaller norm, in comparison with the original unstable discrete solitons. Without the inter-species attraction, $\beta = 0$, IPOS solutions are unstable, except when the Rabi coupling is absent too, $\Omega = 0$, making the system decoupled. On the other hand, CPOS are unstable at $\beta < -1$ and $\Omega \neq 0$. Without the attraction between the components, $\beta = 0$, and for small values of the Rabi coupling parameter ($-1 < \Omega < 0$), CPOS are stable. For higher values of $|\Omega|$, CPOS solutions break into breathing structures. Both components of the complex exhibit the same behavior and evolve into miscible breathers, exchanging the power (norm) in the course of the evolution. All other miscible solutions were found to be unstable.

All inter-site-centered solitons are found to be unstable, as it usually happens in other discrete systems. A trend of the evolution of these unstable modes revealed by the simulations is to end up as on-site breathers with significant emission of matter waves. In particular, the CPIS complexes evolve so that both components exhibit the same behavior and evolve into miscible on-site breathing structures exchanging the power in the course of the evolution. In this case, a part of the emitted matter wave propagates in the form of a new two-component moving complex, see Fig. 4.

Generally, we conclude that all unstable soliton solutions tune their energy, by radiating away a part of it, to the energy corresponding to the miscible on-site solitons existing at the same parameters. The modes evolve as stable on-site breathers. If the radiated energy, transferred to the background, is large enough, as is the case for the CPIS mentioned in the previous paragraph, new moving localized breathing structures can be formed (Fig. 4).

The IMC solutions tend to get destabilized with the increase of the strength of the linear coupling between the components. Usually, they too evolve into miscible breathing modes after radiating away a part of the energy. Stable IMCs feature on-site two-component configurations, see Fig. 2(b). In the area of the system's parameters where the IMCs are stable in the inter-SOC systems, a stable branch of MCs of the on-site type can be found too, which implies bistability between the IMC and MC modes. Then, selection of one of the coexisting solutions is determined by initial conditions. By checking values of the Hamiltonian, we have found that, in the bistability region (the whole gray area in Fig. 6 (b)), the MCs feature smaller energy, hence they realize the ground state of the system. The energy difference between IMC and MC in this case

is smaller for smaller values of C . Similar bistability is found in the inter-SOC system for the parameter set shown in Fig. 6(a) in a narrow area with very small $\Omega \approx 0$ and $0 < C < 0.2$.

Unlike the intra-SOC system, in its inter-SOC counterpart the SOC can induce destabilization of the IMCs (leading to a spontaneous transition from the IMC to an MC) if one sets $\beta = \Omega = C = 0$ in Eq. (7), so that the two components interact solely via the linear SOC terms $\sim \kappa$. This happens in a narrow area of the remaining parameter space.

On the other hand, the SOC affects the threshold of the immiscibility-miscibility transition in both the intra-SOC and inter-SOC systems, in cases of the nonlinear coupling only ($\Omega = 0$), linear coupling only ($\beta = 0$), and when both couplings are present ($\Omega \neq 0, \beta \neq 0$). Figure 6 displays the position of the miscibility threshold, i.e., the curve separating the region of the coexistence of stable IMC and MC, and the region where the IMC is unstable while the MC is stable (as concerns the on-site configurations), in the $(|\Omega|, C)$ parameter plane. In the inter-SOC system [Fig. 6(a)], parameter $\beta = -1$ and $\kappa = 1$ are fixed. In the intra-SOC system, we set $\beta = 0$ and $\kappa = 1$, because for $\beta < -0.5$ stable IMC have not been found [Fig. 6(b)].

Figure 6 demonstrates that the IMC complexes have the largest stability region in the case of $C = 0$, when the usual hopping is negligible, while the SOC terms are present [recall that, as shown in Fig. 1(c), the respective linear spectrum remains meaningful, always featuring the mini-gap]. This case corresponds to the setting when the OL potential is very deep, and, simultaneously, the SOC, induced by the laser beams illuminating the condensate, is strong. Such a setting is feasible, because, in the underlying tight-binding approximation, the hopping coefficient, C in Eqs. (6) and (7), is proportional to the square of the small overlap integral of wave functions (Wannier modes [44]) localized at adjacent sites of the OL, while the scaled SOC coefficient, κ , is proportional to the first power of the same integral. In fact, this limit case emulates the spin-orbit-coupled binary condensate made of *infinitely heavy atoms* (as mentioned above, the case of an infinite particle's mass was recently considered in [15], in the context of a continual model elaborated for the measurement of spin).

Furthermore, in the same limit of $C \rightarrow 0$, the staggering transformation in the form of $\psi_n = i^n \tilde{\psi}_n$ [49], cf. Eq. (8), can be applied to the intra-SOC system, transforming it into a discrete system without the SOC terms, but, effectively, with the hopping coefficients of opposite signs, κ and $-\kappa$, in the two components:

$$\begin{aligned} i \frac{\partial \tilde{\psi}_n^+}{\partial t} &= \kappa(\tilde{\psi}_{n+1}^+ + \tilde{\psi}_{n-1}^+) + (\gamma_1 |\tilde{\psi}_n^+|^2 + \beta |\tilde{\psi}_n^-|^2) \tilde{\psi}_n^+ - \Omega \tilde{\psi}_n^-, \\ i \frac{\partial \tilde{\psi}_n^-}{\partial t} &= -\kappa(\tilde{\psi}_{n+1}^- + \tilde{\psi}_{n-1}^-) + (\beta |\tilde{\psi}_n^+|^2 + \gamma |\tilde{\psi}_n^-|^2) \tilde{\psi}_n^- - \Omega \tilde{\psi}_n^+. \end{aligned} \quad (16)$$

In this way, the model can emulate a two-component BEC with *opposite signs of the effective atomic masses*, which is not possible in the implementation of the BEC.

Continuing the consideration of IMC modes in the intra-SOC system, we outline typical instability-development scenarios for them (similar scenarios are produced by the

inter-SOC system). Unstable on-site IMCs may actually be very robust overall, evolving into localized breathing miscible structures, see Fig. 7. In that case, the two components of the on-site IMC evolve into miscible breathing structures, which exchange the norm in the course of the evolution.

Figure 8 illustrates the dynamics of an unstable inter-site IMC. In the course of the evolution, a large share of the norm is radiated away, and the formation of irregular localized patterns is observed in a neighborhood of the initial position of the components.

All the localized complexes considered above are generated in the semi-infinite gap, in terms of the spectra of the linearized systems. It remains to briefly describe what happens when a mini-gap opens at $|\Omega| > 2C$, as shown in Figs. 1(b) and (c). In that gap, we have found miscible CPOS and CPIS complexes, which resemble similar complexes found in the semi-infinite gap, see Fig. 3. Only the CPOS complexes may be stable in certain parameter areas inside the mini-gap. All other structures are highly unstable in this case.

To summarize this section, the stable on-site localized MCs (miscible complexes) can be created in the large area of the parameter space in the two-component SOC-BEC system. On the other hand, stable IMCs (immiscible complexes) were found only in a narrow parametric area. The latter one is often a bistability region, where the system supports both the IMC and MC stable complexes (which is usually not possible in the free space [30]). Unstable IMCs, as well as unstable inter-site MCs, evolve into breathing miscible states, emitting matter waves away. These conclusions pertain to both the intra-SOC and inter-SOC systems considered. Thus, we conclude that, in general, all inter-species couplings, linear (SOC) and attractive nonlinear ones, favor miscible states.

4. Conclusions

We have introduced a discrete one-dimensional model of SOC (spin-orbit-coupled) binary BEC trapped in a deep OL potential. Two systems were considered, of the intra-SOC and inter-SOC types, in which the SOC terms, represented by the discrete version of the first spatial derivatives, act, respectively, inside of each component corresponding to the dressed atomic state, or couple the different components. Each system includes attractive intra- and inter-species cubic interactions (repulsive interactions can be transformed into the same form by means of staggering). It has been demonstrated that both systems support two distinct types of discrete soliton complexes, miscible and immiscible ones, depending on values of the systems' parameters. The transition between the two types of the complexes can be controlled by the SOC strength. As usual, only on-site-centered modes may be stable. The SOC terms may open up a mini-gap in the systems' spectrum, where stable miscible on-site soliton complexes exist too.

New possibilities offered by these settings are scenarios for the emulation of SOC binary condensates built of infinitely heavy atoms, as well as of the binary BEC with

effective atomic masses which have opposite signs. Both settings, that correspond to the limit when the usual hoppings are negligible, while the SOC keeps acting, are obviously unavailable in the direct realization of BEC.

To continue the present analysis, it may be interesting to consider bound states of the discrete solitons, as well as their mobility. A challenging problem is to extend the analysis to the 2D setting, where it has been recently demonstrated that the SOC, in the combination with the nonlinear attraction, supports stable bright solitons in the in the presence of the OL potential [27, 30], as well as in *free space* [28, 30] (without the SOC, all 2D solitons sustained by the cubic attractive interaction in the free space are unstable against the critical collapse).

Acknowledgments

P.P.B., G.G., J.P., A.M., and Lj.H. acknowledge support from the Ministry of Education and Science of Serbia (Project III45010). B.A.M. appreciates valuable discussions with H. Sakaguchi, V. V. Konotop, Y. V. Kartashov, and L. Salasnich.

References

- [1] Bloch I, Dalibard J and Zwerger W 2008 *Rev. Mod. Phys.* **80**; Dalibard J, Gerbier F, Juzeliūnas G and Ohberg P 2011 *Rev. Mod. Phys.* **83** 1523
- [2] Dresselhaus G 1955 *Phys. Rev.* **100** 580
- [3] Bychkov Y A and Rashba E I 1984 *J. Phys. C* **17** 6039
- [4] Xiao D, Chang M C and Niu Q 2010 *Rev. Mod. Phys.* **82** 1959
- [5] Hasan M and Kane C L 2010 *Rev. Mod. Phys.* **82** 3045
- [6] Žutić I, Fabian J and Das Sarma S 2004 *Rev. Mod. Phys.* **76** 323
- [7] Quay C H L, Hughes T L, Sulpizio J A, Pfeiffer L N, Baldwin K W, West K W, Goldhaber-Gordon D and de Picciotto R 2010 *Nat. Phys.* **6** 336
- [8] Bloch I, Dalibard J and Nascimbène S 2012 *Nat. Phys.* **8** 267 (2012); Houck A A, Tureci H E and Koch J. 2012 *Nat. Phys.* **8** 292; Johanning M, Varon A F and Wunderlich C 2009 *J. Phys. B: At. Mol. Opt. Phys.* **42** 154009
- [9] Campbell D L, Juzeliūnas G and Spielman I B 2011 *Phys. Rev. A* **84**, 025602
- [10] Lin Y J, Jimenez-Garcia K and Spielman I B 2011 *Nature* **471** 83
- [11] Galitski V and Spielman I B 2013 *Nature* **494** 49
- [12] Zhang J-Y, Ji S-C, Chen Z, Zhang L, Du Z-D, Yan B, Pan G-S, Zhao B, Deng Y-J, Zhai H, Chen S and Pan J-W 2012 *Phys. Rev. Lett.* **109** 115301
- [13] Fisher M P A, Weichman P B, Grinstein G and Fisher D S 1989 *Phys. Rev. B* **40** 546; Greiner M, Mandel O, Esslinger T, Hansch T W and Bloch I 2002 *Nature* **415** 39; Erhard M, Schmaljohann H, Kronjäger J, Bongs K and Sengstock K 2004 *Phys. Rev. A* **69** 032705
- [14] Zhang Y, Mao L and Zhang C 2012 *Phys. Rev. Lett.* **108** 035302; Zhang Y, Chen G and Zhang C 2013 *Sci. Rep.* **3** 1937; Zhang Y, Song Sh and Liu W 2014 *Sci. Rep.* **4** 4992
- [15] Sherman E Ya and Sokolovski D 2014 *New J. Phys.* **16** 015013
- [16] Liu X J, Borunda M F, Liu X and Sinova J 2009 *Phys. Rev. Lett.* **102** 046402
- [17] Wang P, Yu Z Q, Fu Z, Miao J, Huan L, Chai S, Zhai H and Zhang J 2012 *Phys. Rev. Lett.* **109** 095301; Cheuk L W, Sommer A T, Hadzibabic Z, Yefsah T, Bakr W S and Zwierlein M W 2012 *Phys. Rev. Lett.* **109** 095302
- [18] Zhai H 2012 *Int. J. Mod. Phys. B* **26** 1230001

- [19] Stenger J, Inouye S, Stamper-Kurn D M, Miesner H J, Chikkatur A P and Ketterle W 1998 *Nature* **396** 345
- [20] Chang M S, Hamley C D, Barrett M D, Sauer J A, Fortier K M, Zhang W, You L and Chapman M S 2004 *Phys. Rev. Lett.* **92** 140403
- [21] Ho T L 1998 *Phys. Rev. Lett.* **81** 742
- [22] Wang C, Gao C, Jian C M and Zhai H 2010 *Phys. Rev. Lett.* **105** 160403; Zezyulin D A, Driben R, Konotop V V and Malomed B A 2013 *Phys. Rev. A* **88** 013607
- [23] Li Y, Pitaevskii L P and Stringari S 2012 *Phys. Rev. Lett.* **108** 225301
- [24] Achilleos V, Frantzeskakis D J, Kevrekidis P G and Pelinovsky D E 2013 *Phys. Rev. Lett.* **110** 264101
- [25] Kartashov Y V, Konotop V V and Abdullaev F Kh 2013 *Phys. Rev. Lett.* **111** 060402
- [26] Xu Y, Zhang Y. and Wu B 2013 *Phys. Rev. A* **87** 013614; Salasnich L and Malomed B A *Phys. Rev. A* **87** 063625
- [27] Lobanov V E, Kartashov Y V and Konotop V V 2014 *Phys. Rev. Lett.* **112** 180403
- [28] Sakaguchi H, Li B and Malomed B A 2014 *Phys. Rev. E* **89** 032920
- [29] Salasnich L, Cardoso W. B. and Malomed B A 2014 *Phys. Rev. A* **90** 033629
- [30] Sakaguchi H and Malomed B A 2014 *Phys. Rev. E* **90** 062922
- [31] Sakaguchi H and Li B 2013 *Phys. Rev. A* **87** 015602
- [32] Zhang Y and Zhang Ch 2013 *Phys. Rev. A* **87** 023611
- [33] Larson J, Martikainen J P, Collin A and Sjöqvist E 2010 *Phys. Rev. A* **82** 043620
- [34] Stanescu T D, Galitski V, Vaishnav J Y, Clark Ch W and Das Sarma S 2009 *Phys. Rev. A* **79** 053639
- [35] C. J. Myatt, E. A. Burt, R. W. Ghrist, E. A. Cornell, and C. E. Wieman, *Phys. Rev. Lett.* **78**, 586 (1997).
- [36] Pu H and Bigelow N P 1998 *Phys. Rev. Lett.* **80** 1130
- [37] Hall D S, Matthews M R, Ensher J R, Wieman C E and Cornell E A 1998 *Phys. Rev. Lett.* **81** 1539
- [38] Inouye S, Andrews M R, Stenger J, Miesner H J, Stamper-Kurn D M and Ketterle W 1998 *Nature* **392** 151
- [39] Timmermans P, Tommasini P, Hussein M and Kerman A 1999 *Phys. Rep.* **315** 199
- [40] Fedichev P O, Kagan Yu, Shlyapnikov G V and Walraven J T M 1996 *Phys. Rev. Lett.* **77** 2913
- [41] Theis M, Thalhammer G, Winkler K, Hellwig M, Ruff G, Grimm R and Denschlag J H 2004 *Phys. Rev. Lett.* **93** 123001
- [42] Merhasin I M, Malomed B A and Driben R 2005 *J. Phys. B: At. Mol. Opt. Phys.* **38** 877
- [43] Gligorić G, Maluckov A, Stepić M, Hadžievski Lj and Malomed B A 2010 *Phys. Rev. A* **82** 033624
- [44] Trombettoni A and Smerzi A 2001 *Phys. Rev. Lett.* **86** 2353; Abdullaev F Kh, Baizakov B B, Darmanyan S A, Konotop V V and Salerno M 2001 *Phys. Rev. A* **64** 043606; Alfimov G L, Kevrekidis P G, Konotop V V and Salerno M 2002 *Phys. Rev. E* **66** 046608; Carretero-González R and Promislow K 2002 *Phys. Rev. A* **66** 033610; Efremidis N K and Christodoulides D N 2003 *Phys. Rev. A* **67** 063608; Maluckov A, Hadžievski Lj, Malomed B A and Salasnich L 2008 *Phys. Rev. A* **78** 013616
- [45] Kevrekidis P G 2009 *The Discrete Nonlinear Schrödinger Equation: Mathematical Analysis, Numerical Computations, and Physical Perspectives* (Springer: Berlin and Heidelberg)
- [46] Gligorić G, Maluckov A, Hadžievski Lj and Malomed B A 2008 *Phys. Rev. A* **78** 063615
- [47] Konotop V V and Salerno M 2002 *Phys. Rev.* **65** 021602; Louis P J Y, Ostrovskaya E A and Kivshar Y S 2005 *Phys. Rev. A* **71** 023612; Porter M, Kevrekidis P G, Carretero-González R and Frantzeskakis D J 2006 *Phys. Lett. A* **352** 210; Yagasaki K, Merhasin I M, Malomed B A, Wagenknecht T and Champneys A R 2006 *EPL* **74** 1006; Sukhorukov A A 2006 *Phys. Rev. Lett.* **96** 113902
- [48] Gligorić G, Maluckov A, Hadžievski Lj and Malomed B A 2014 *Chaos* **24** 023124
- [49] Kevrekidis P G, Malomed B A and Musslimani Z 2013 *Eur. Phys. J. D* **67** 412

- [50] Lederer F, Stegeman G I, Christodoulides D N, Assanto G, Segev M. and Silberberg Y 2008 *Phys. Rep.* **683** 1
- [51] Gligorić G, Maluckov A, Hadžievski Lj, Slepyan G Ya and Malomed B A 2013 *Phys. Rev. B* **88** 155329

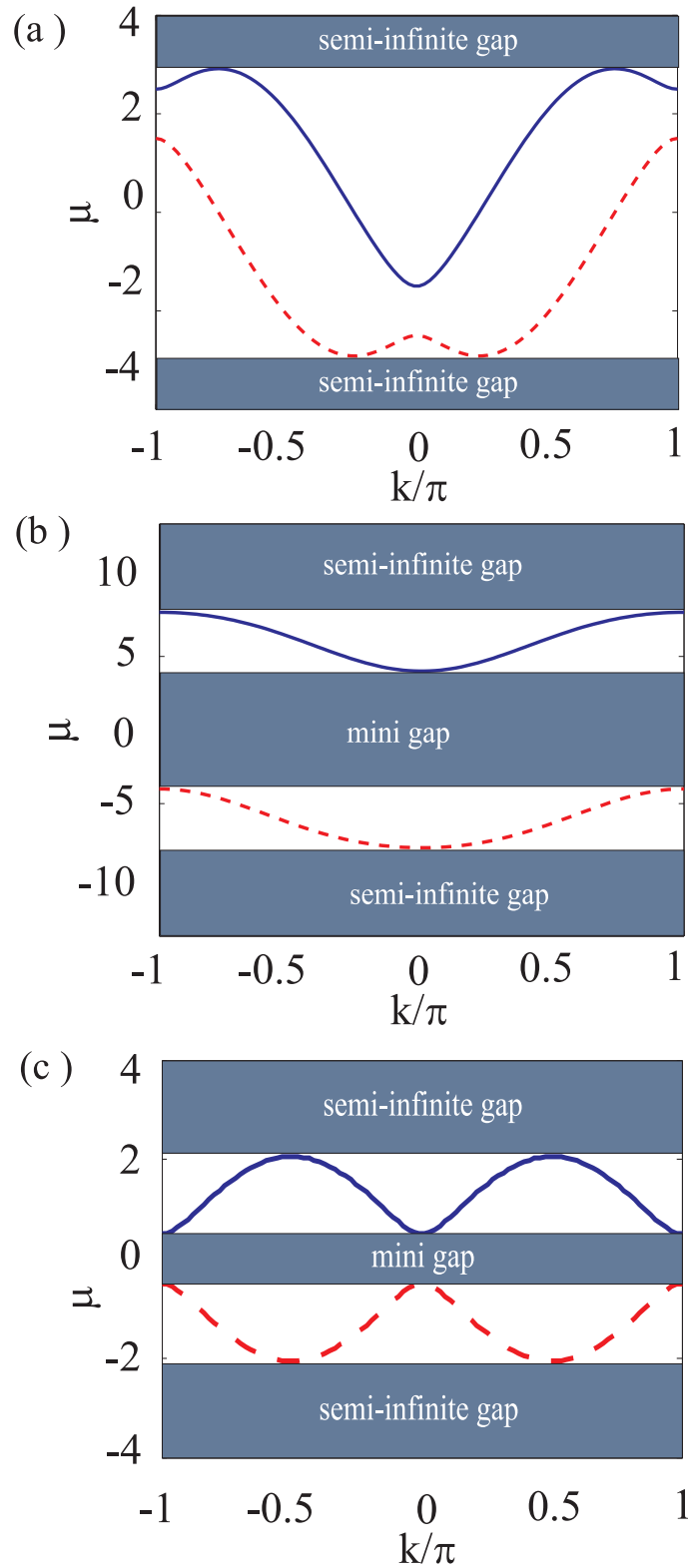


Figure 1. (Color online) Dispersion curves, as given by Eq. (14), for (a) $\Omega = -0.5$, $C = 1$; (b) $\Omega = -6$, $C = 1$; and (c) $\Omega = -0.5$, $C = 0$. In all the plots, $\kappa = 1$. At $|\Omega| > 2C$, the mini-gap Eq. (15) opens up around $\mu = 0$. This figure corresponds to both systems considered here, of the intra-SOC and inter-SOC types, i.e., given by Eqs. (6) and (7), respectively.

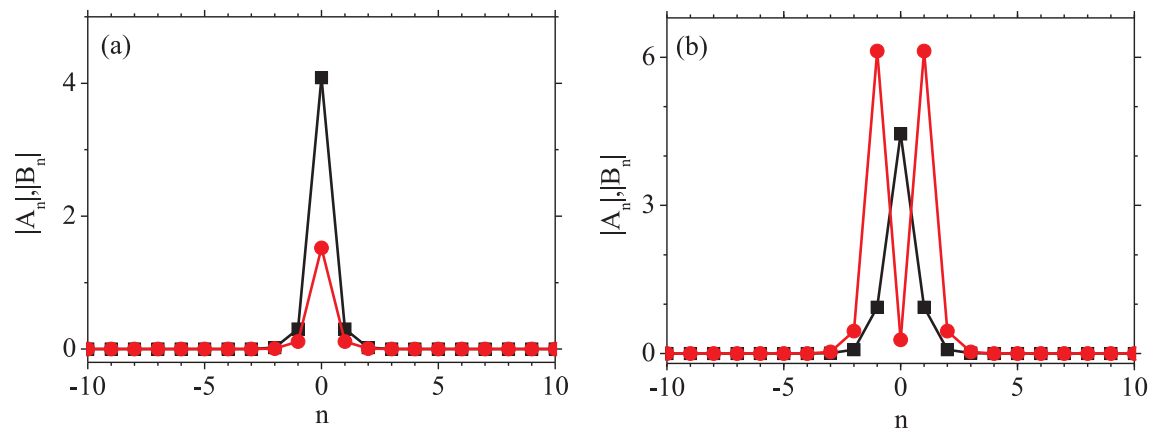


Figure 2. (Color online) Panels (a) and (b) display typical shapes of the discrete miscible and immiscible complexes (MCs and IMCs), respectively. Black (squares) and red (circles) lines denote, severally, components A_n and B_n . The respective parameters in Eq. (12) are $\kappa = 1$, $\gamma_1 = -1$, $\gamma = -0.5$, $\beta = -1$, $\Omega = -2$, $\mu = -19.4$, $C = 1$.

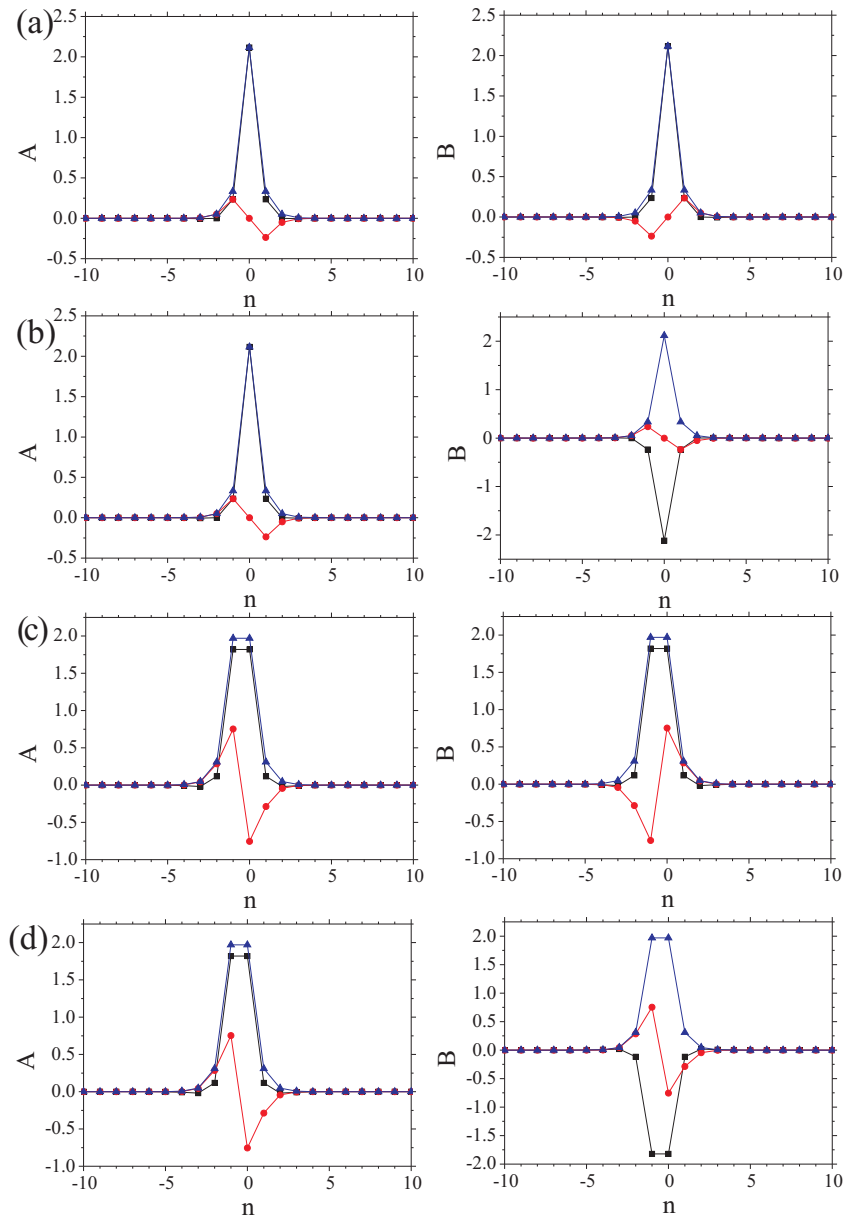


Figure 3. (Color online) Examples of discrete two-component solitons of the miscible type: (a) an IPOS complex, (b) a CPOS complex, (c) an IPIS complex, and (d) a CPIS complex. Black (squares), red (circles), and blue (triangles) lines depict real and imaginary parts and the absolute value of the fields, respectively. The parameters are $\kappa = 1$, $\gamma = \gamma_1 = -1$, $C = 1$, $\mu = -9.4$.

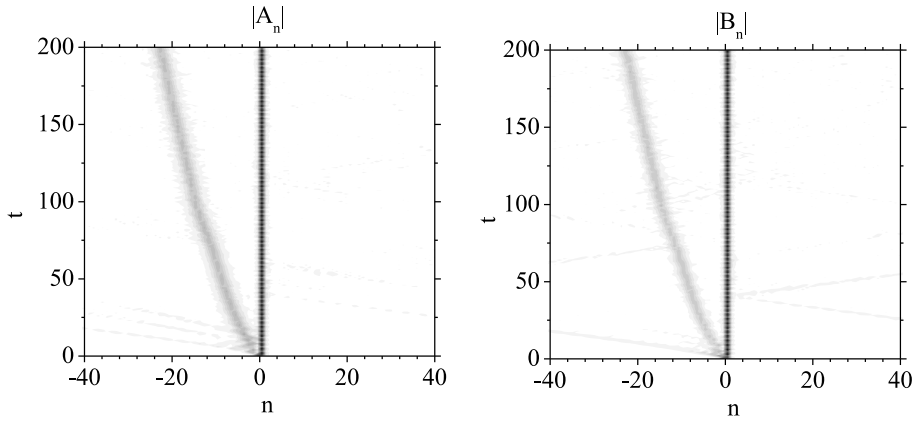


Figure 4. The evolution of two components of an inter-site CPIS mode with $\mu = -9.4$, $\kappa = 1$, $\gamma = -0.5$, $\gamma_1 = -1$, $\beta = -2$, $\Omega = -0.5$, and $C = 1$. Both components break into a trapped on-site mode and a moving one. Initial small random perturbations are added to the solutions to catalyze the onset of the instability.

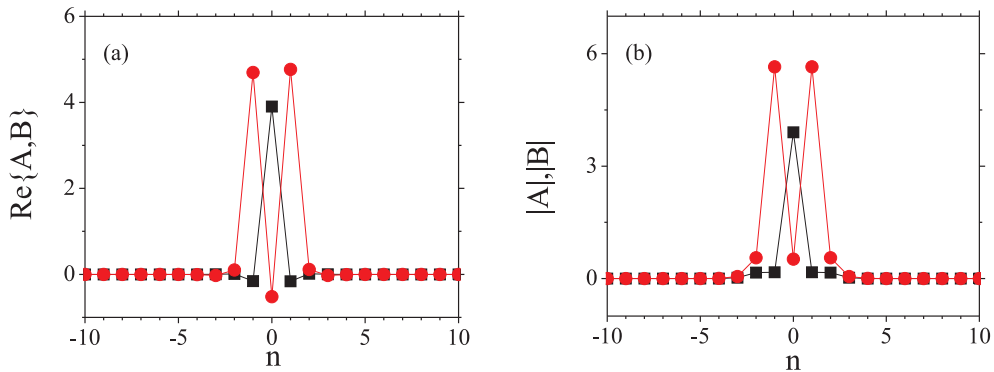


Figure 5. (Color online) An example of a stable IMC (immiscible complex): (a) real parts of its two components; (b) the corresponding absolute values. The parameters are: $\Omega = -4$, $\gamma_1 = -1$, $\gamma = -0.5$, $\beta = -5$, $\mu = -16$, $\kappa = 1$ and $C = 1$. Black lines with squares and red lines with circles are associated with components A and B , respectively.

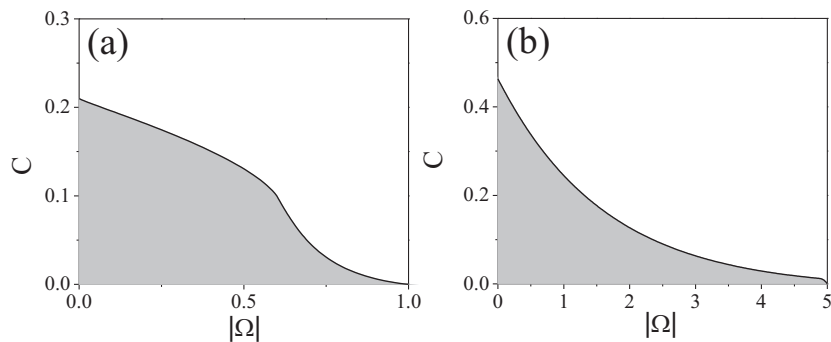


Figure 6. (Color online) The transition from stable (gray areas) to unstable (white areas) IMC in the $(|\Omega|, C)$ plane: (a) in the inter-SOC system [Eq. (7) with $\beta = -1$], and (b) in the intra-SOC one [Eq. (6), with $\beta = 0$]. Other parameters are $\gamma = \gamma_1 = -1$, and $\kappa = 1$. In the area with small $|\Omega|$ in the grey area in plot (a) stable IMC and MC can exist. While in the plot (b) in the entire gray area both stable IMCs and MCs can be created (bistability regions). Those IMCs which are unstable (white areas in figure) spontaneously evolve into stable MC breathers, after radiating away a part of the initial norm.

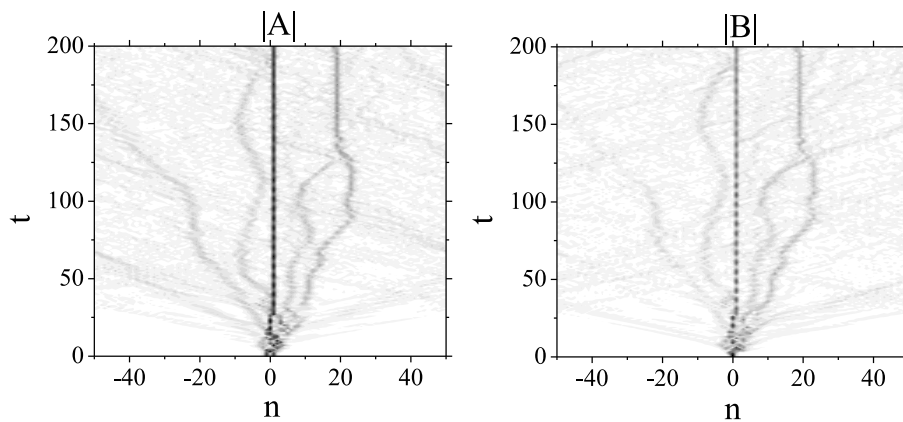


Figure 7. The evolution of an unstable immiscible complex (IMC) in the intra-SOC system with $\mu = -19.4$, $\kappa = 1$, $\gamma = -0.5$, $\gamma_1 = -1$, $\beta = -1$, $\Omega = -2$, and $C = 1$. Initial small random perturbations were added to the immiscible localized complex.

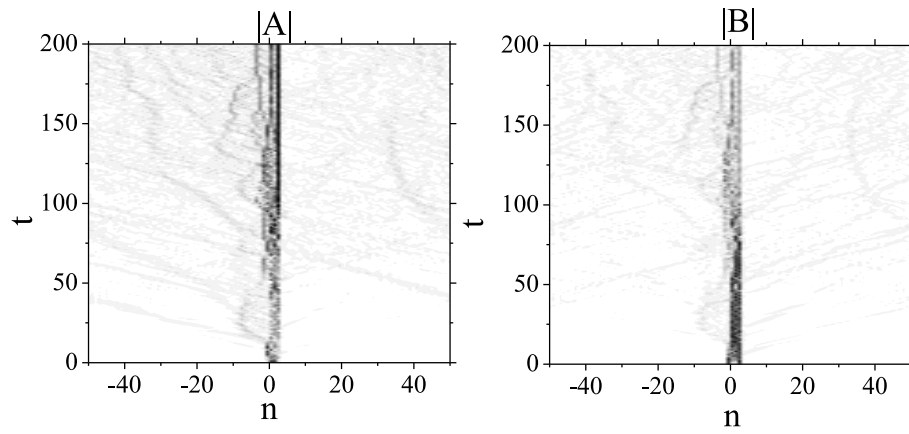


Figure 8. (Color online) The evolution of an unstable inter-site IMC in the intra-SOC system. The parameters are the same as in Fig. 7.